



RESEARCH LETTER

10.1002/2016GL071515

Key Points:

- The 1997/1998 event is the strongest EP El Niño, while the 2015/2016 event is the strongest mixed EP and CP El Niño ever recorded
- The two events exhibit subtle differences in their equatorial SST evolution that reflects fundamental differences in the underlying dynamics
- The SST differences led to large differences in tropical convection, resulting in different impacts on North American climate

Supporting Information:

- Supporting Information S1

Correspondence to:

H. Paek,
paekh@uci.edu

Citation:

Paek, H., J.-Y. Yu, and C. Qian (2017), Why were the 2015/2016 and 1997/1998 extreme El Niños different?, *Geophys. Res. Lett.*, 44, doi:10.1002/2016GL071515.

Received 10 OCT 2016

Accepted 6 FEB 2017

Accepted article online 8 FEB 2017

Why were the 2015/2016 and 1997/1998 extreme El Niños different?

Houk Paek¹ , Jin-Yi Yu¹ , and Chengcheng Qian²

¹Department of Earth System Science, University of California, Irvine, California, USA, ²Department of Marine Technology, College of Information Science and Engineering, Ocean University of China, Qingdao, China

Abstract Subtle but important differences are identified between the 1997/1998 and 2015/2016 extreme El Niños that reflect fundamental differences in their underlying dynamics. The 1997/1998 event is found to evolve following the eastern Pacific El Niño dynamics that relies on basin-wide thermocline variations, whereas the 2015/2016 event involves additionally the central Pacific (CP) El Niño dynamics that depends on subtropical forcing. The stronger CP dynamics during the 2015/2016 event resulted in its sea surface temperature (SST) anomalies lingering around the International Date Line during the decaying phase, which is in contrast to the retreat of the anomalies toward the South American Coast during the decaying phase of the 1997/1998 event. The different SST evolution excited different wave trains resulting in the western U.S. not receiving the same above-normal rainfall during the 2015/2016 El Niño as it did during the 1997/1998 El Niño. Ensemble model experiments are conducted to confirm the different climate impacts of the two El Niños.

1. Introduction

The recent 2015/2016 El Niño is one of the strongest events ever recorded and has been generally considered to be similar and comparable to another extreme event—the 1997/1998 El Niño. The strengths of these two extreme events are comparable with their maximum sea surface temperature (SST) anomalies both reaching about 3.5°C. Their evolution is also seemingly similar, as during both events SST anomalies spread mainly from the South American Coast toward the International Date Line during their developing stages that began in late boreal spring (Figures 1a and 1b). However, the two events began to differ from each other in their decaying phases, during which SST anomalies retracted to the South American Coast beginning in January 1998 for the 1997/1998 event but stayed in the equatorial central Pacific from late winter to spring of 2016 for the 2015/2016 event. This difference indicates that the underlying dynamics of these two events may not be the same.

Although each El Niño–Southern Oscillation (ENSO) event is unique, recent studies have broadly classified them into two different types: one has its most prominent equatorial Pacific SST anomalies extending westward from the South American Coast and the other has its most prominent SST anomalies confined around the International Date Line or extending toward eastern Pacific [Larkin and Harrison, 2005; Yu and Kao, 2007; Ashok et al., 2007; Kao and Yu, 2009; Kug et al., 2009]. These two types are now, respectively, referred to as the eastern Pacific (EP) ENSO and central Pacific (CP) ENSO [Yu and Kao, 2007; Kao and Yu, 2009] to emphasize the different locations of their SST anomalies. The EP ENSO has been suggested to be generated by the traditional ENSO dynamics with SST anomalies in the equatorial eastern Pacific being controlled by the thermocline feedback [e.g., Wyrtki, 1975; Suarez and Schopf, 1988; Battisti and Hirst, 1989; Jin, 1997], whereas the generation mechanism of CP ENSO has been suggested to be less sensitive to the thermocline variations but involves the zonal advective feedback [Kug et al., 2009; Yu et al., 2010; Capotondi, 2013] and forcing from the subtropical atmosphere. The subtropical atmospheric fluctuations, particularly those associated with the North Pacific Oscillation (NPO) [Walker and Bliss, 1932; Rogers, 1981], can first induce positive SST anomalies off Baja California during boreal winter [e.g., Vimont et al., 2003; Chang et al., 2007; Yu and Kim, 2011], which then spread southwestward in the following seasons through subtropical atmosphere–ocean coupling—assuming a pattern similar to the so-called Pacific Meridional Mode (PMM) [Chiang and Vimont, 2004]—and reach the tropical central Pacific to give rise to a CP type of El Niño [Yu et al., 2010, 2012a, 2015; Kim et al., 2012; Lin et al., 2015].

During the most recent two decades, the CP type of El Niño not only emerged more frequently [Ashok et al., 2007; Kao and Yu, 2009; Kug et al., 2009] but also intensified [Lee and McPhaden, 2010]. Most of the El Niño events that have occurred so far in the 21st century were of the CP type [Lee and McPhaden, 2010; Yu et al.,

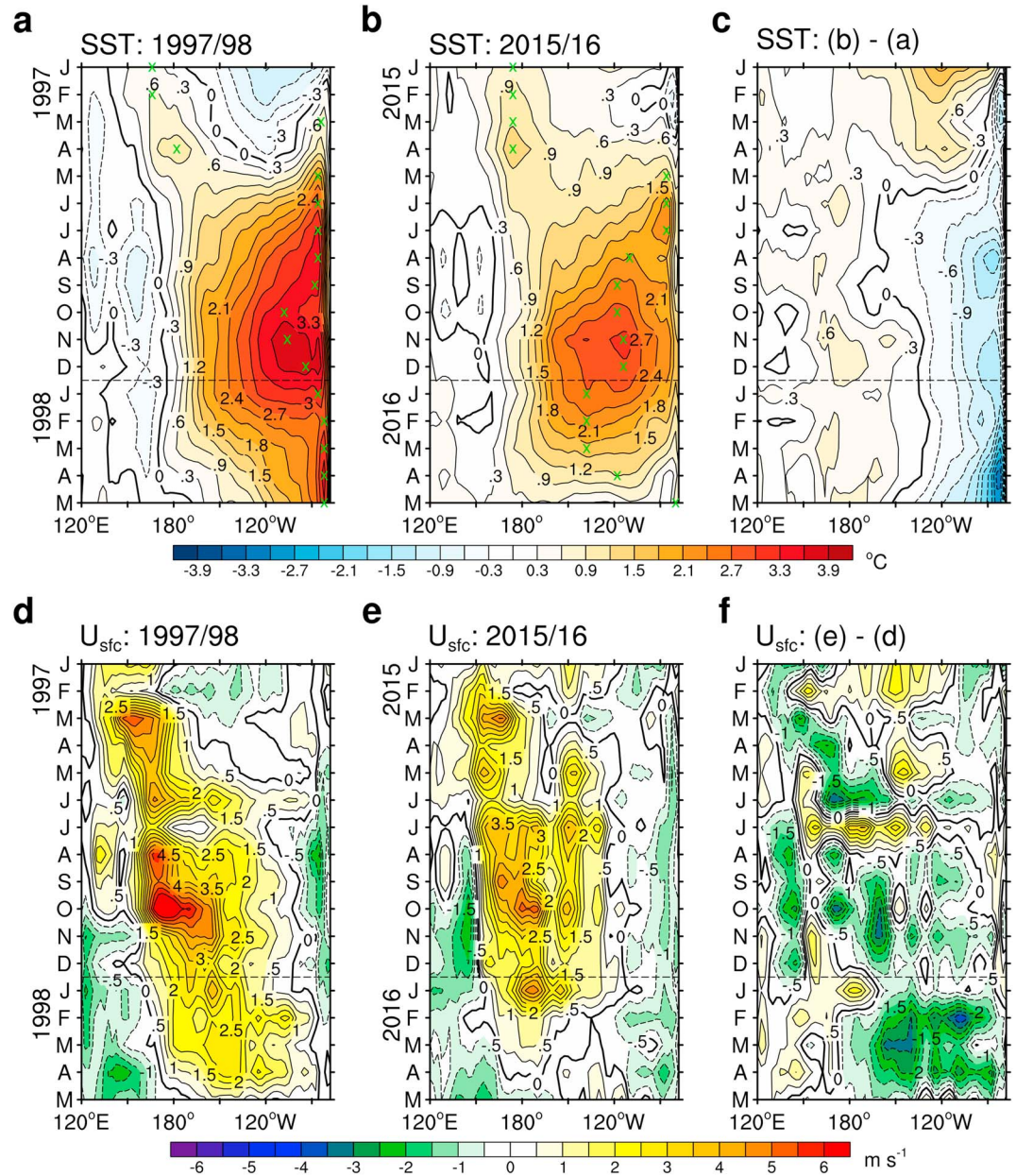


Figure 1. The evolution of equatorial SST anomalies averaged over 5°S–5°N for (a) the 1997/1998 event, (b) the 2015/2016 event, and (c) their difference. The green crosses indicate local maxima. (d–f) As in Figures 1a–1c but for the surface westerly wind (U_{sfc}) anomalies.

2012b, 2015]. Nevertheless, the latest 2015/2016 El Niño seems like a conventional EP type, which appears to interrupt the increased frequency of occurrence trend of the CP El Niño. Here we use the view of the two types of ENSO to show that the trend did not get interrupted. The 2015/2016 El Niño is actually not a pure EP type but a mixture of the EP and CP types, which makes it different from the 1997/1998 El Niño which is more of a pure EP type. The difference in the El Niño type between these two events is one of the possible reasons why the impacts of these two comparable extreme events on North America climate are different.

2. Data and Indices

In this study, the following observation/reanalysis products were used as follows: (1) the National Oceanic and Atmospheric Administration’s (NOAA) Extended Reconstructed Sea Surface Temperature data set

[Smith *et al.*, 2008], (2) the National Centers for Environmental Prediction/National Center for Atmospheric Research's (NCEP/NCAR) Reanalysis data set [Kalnay *et al.*, 1996], (3) NOAA's Precipitation Reconstruction data set [Chen *et al.*, 2002], and (4) the NCEP Global Ocean Data Assimilation System (GODAS) reanalysis data set [Saha *et al.*, 2006]. All the data sets were downloaded from www.esrl.noaa.gov/psd/. We analyzed monthly data for the period 1961–2016 (except for the GODAS data set that is available for the period 1981–2016) and calculated the anomalies by removing the mean seasonal cycles for the period 1981–2010. We obtained similar results (not shown) when repeating the same analyses with the Climate Prediction Center's Merged Analysis of Precipitation data set [Xie and Arkin, 1997], the Hadley Centre's Sea Ice and sea surface temperature data set [Rayner *et al.*, 2003], and the European Centre for Medium-Range Weather Forecasts' ERA-Interim data set [Dee *et al.*, 2011].

We also used several climate indices in the analyses. To identify the EP and CP ENSO events, we first removed SST anomalies regressed onto the Niño4 index (SST anomalies averaged over 5°S–5°N, 160°E–150°W; i.e., the anomalies representing the CP ENSO influence) or the Niño1 + 2 index (10°S–0°, 80°–90°W; i.e., the anomalies representing the EP ENSO influence) from the original SST anomalies. The leading principal components (PCs) from an empirical orthogonal function (EOF) analysis of the Niño4-removed SST anomalies and the Niño1 + 2-removed SST anomalies in the tropical (20°S–20°N) Pacific are referred to as the EP index (EPI) and CP index (CPI), respectively [Kao and Yu, 2009; Yu and Kim, 2010]. To quantify the subtropical atmospheric forcing, a NPO index was obtained as the second leading PC of an EOF analysis of sea level pressure anomalies over the North Pacific (20°–60°N, 120°E–80°W). To quantify the strength of the atmosphere-ocean coupling in the subtropical Pacific, a PMM index was obtained as the leading PCs of a singular value decomposition (SVD) analysis of the cross covariance between SST and surface zonal and meridional wind anomalies over the eastern Pacific (20°S–30°N, 175°E–95°W). Before the SVD analysis, we subtracted the regressions onto the cold tongue index (CTI; SST anomalies averaged over 6°S–6°N, 180°–90°W) from the original SST and wind anomalies to remove the ENSO influence following Chiang and Vimont [2004]. The two leading PCs are referred to as the PMM SST index and the PMM wind index, respectively.

3. Results

3.1. Contrasting the 1997/1998 and 2015/2016 El Niño Events

As mentioned, positive SST anomalies during the 1997/1998 El Niño (Figure 1a) first appeared off the South American Coast in May 1997 and later spread westward during the developing phase of the event, reached their peak intensity in November 1997, and retreated back to the Coast during the decaying phase in boreal spring 1998. This evolution matches that of the typical EP type of El Niño [Kao and Yu, 2009]. During the 2015/2016 El Niño (Figure 1b), warm anomalies also first appeared off the South American Coast during boreal spring 2015 then extended westward during the developing phase of the event and reached their peak intensity in November 2015. The peak values of the CTI exceeded three standard deviations for both events. Specifically, the CTI reached a peak of 2.3°C for the 1997/1998 event and 2.2°C for the 2015/2016 event. As a result, these two events are considered the two strongest El Niño events ever recorded (http://www.cpc.ncep.noaa.gov/products/analysis_monitoring/ensostuff/ensoyears.shtml) and are referred to as “very strong,” or “extreme” El Niño events. However, the maximum SST anomalies during the 2015/2016 event were displaced westward compared to those during the 1997/1998 event (Figure 1c). This difference was particularly large during the decay phase. Consistent with the westward displaced SST anomalies, surface westerly wind anomalies during the 2015/2016 event were confined to the west of 120°W (Figure 1e). In contrast, westerly wind anomalies during the 1997/1998 event (Figure 1d) prevailed across most of the equatorial Pacific (roughly from 150°E to 90°W), which is consistent with the typical pattern of westerly wind anomalies identified for the EP El Niño [Kao and Yu, 2009]. The peak magnitude of the westerly wind anomalies during the 2015/2016 event (2.6 m s^{-1}) was about 35% smaller than during the 1997/1998 event (3.5 m s^{-1}) (Figure 1f).

The location of SST anomalies implies that the 2015/2016 event may have contained stronger spatial pattern and evolution of the CP type of El Niño than the 1997/1998 event. To examine this possibility, we compared the CTI, EPI, and CPI for these two events (Figures 2a and 2b). The CTI evolution is similar for these two events, as the CTI began to increase to larger positive values during the boreal springs of the El Niño years, reached a peak during the winters, and decayed during the following springs. Based on the CTI, the 2015/2016 event is similar to the 1997/1998 event. The EPI and CPI, however, paint a very different picture. During the 1997/1998

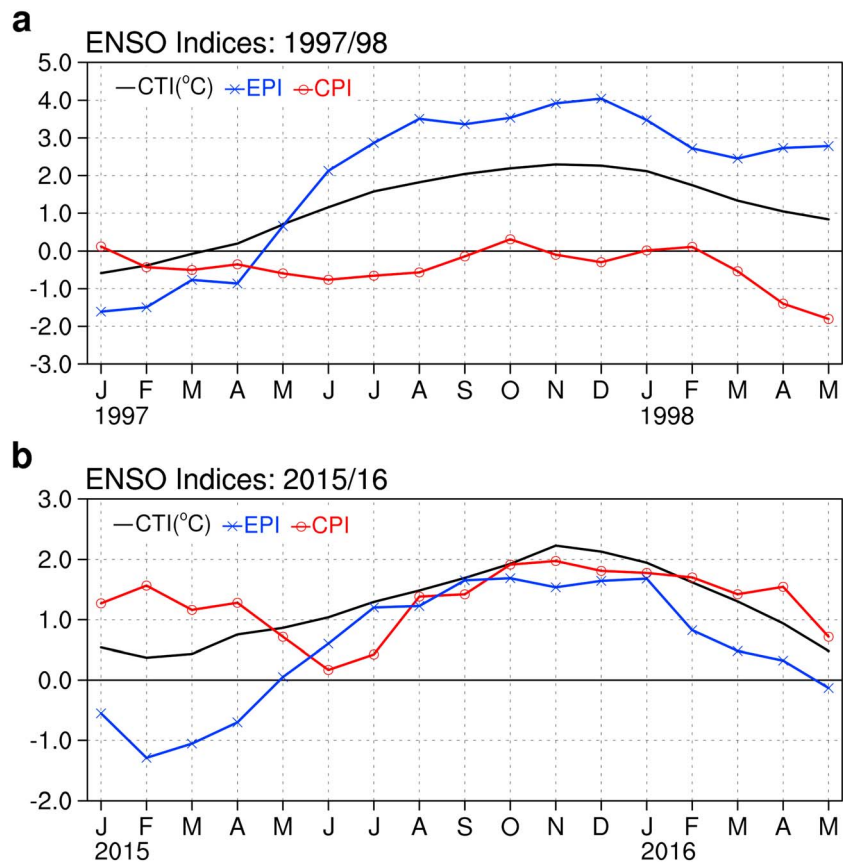


Figure 2. The evolution of three indices, the CTI (i.e., representing an ENSO), the EPI (i.e., representing an EP ENSO), and the CPI (i.e., representing a CP ENSO) for (a) the 1997/1998 event and (b) the 2015/2016 event.

event (Figure 2a), the EPI switched from negative values during boreal winter 1996 to positive values in late spring 1997, reached a peak in December 1997 with large positive values that persisted into the following spring, while the values of the CPI were small throughout the event. It is obvious that the EPI dominates the CPI throughout the 1997/1998 event. Thus, this event should be recognized as a pure EP El Niño. The evolution of the EPI during the 2015/2016 event (Figure 2b) is similar to that of the 1997/1998 event, except that the 2015/2016 event had smaller amplitudes and decayed faster. However, the CPI displays large positive values throughout the 2015/2016 event that were not seen in the 1997/1998 event. During the peak phase of the 2015/2016 event, the EPI and CPI values are comparable (1.7 and 2.0, respectively). This analysis suggests that the 2015/2016 event is not a pure EP El Niño but an equal mixture of the EP and CP types of El Niño. Based on the values of EPI and CPI, the 2015/2016 event became dominated by the CP El Niño dynamics after October 2015, which may be the reason why its SST evolution differed significantly from the 1997/1998 event during its decaying phase.

By examining the indices for the 18 El Niño events observed since 1960 (Figure S1 in the supporting information), we find that the 2015/2016 event is the strongest mixed type of El Niño ever recorded, whereas the 1997/1998 event is the strongest pure EP type of El Niño. Our analysis also finds the 2009/2010 event to be the strongest pure CP type of El Niño. To insure that our identification of the types of the 1997/1998 and 2015/2016 El Niño events are not due to the use of the EPI and CPI, we also used the indices defined in Takahashi *et al.* [2011] for classifying the two types of El Niño and found similar results (not shown).

3.2. Underlying El Niño Dynamics of the 1997/1998 and 2015/2016 Events

As mentioned above, the EP El Niño dynamics is best represented by thermocline variations propagating along the equatorial Pacific. The 1997/1998 event (Figure 3a) was characterized by a strong basin-wide propagation of the thermocline anomalies, during which positive anomalies propagated from the tropical

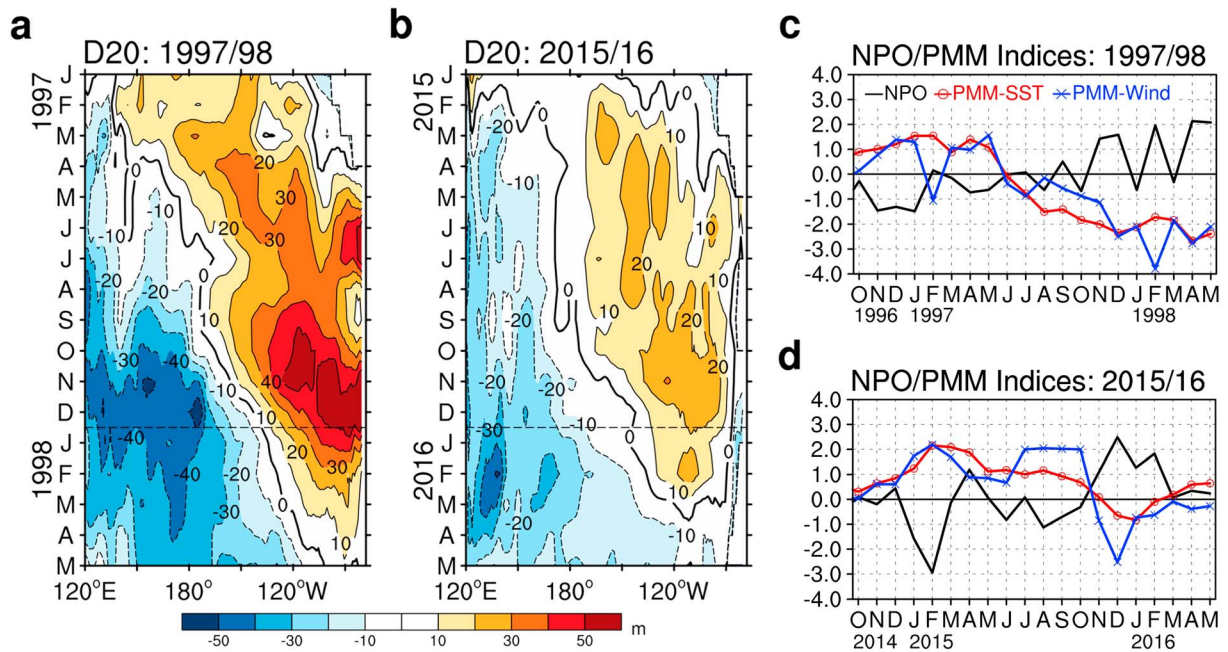


Figure 3. The evolution of the equatorial 20°C isotherm depth (D20; representing the thermocline) anomalies averaged over 5°S–5°N, a proxy for the EP El Niño dynamics for (a) the 1997/1998 event and (b) the 2015/2016 event. The NPO and PMM indices—a proxy for the CP El Niño dynamics—for (c) the 1997/1998 event and (d) the 2015/2016 event.

western to eastern Pacific during its developing phase, intensified during its peak phase, followed by negative anomalies propagating from the western Pacific during its decaying phase. This analysis indicates that the traditional delayed oscillator mechanism [Suarez and Schopf, 1988] is at work during the 1997/1998 event. The thermocline anomalies during the 2015/2016 event are much weaker than those during the 1997/1998 event (Figure 3b), despite the fact that the two events have comparable SST anomalies. The maximum value of the thermocline anomalies (averaged over 120°E–90°W) during boreal summer is 14.3 m for the 1997/1998 event but only 4.6 m for the 2015/2016 event. The EP El Niño dynamics is apparently weaker during the 2015/2016 event than during the 1997/1998 event.

The onset of a CP El Niño is known to be related to subtropical atmospheric forcing associated with the negative phase of the NPO [e.g., Yu and Kim, 2011] and the subtropical Pacific coupling associated with the PMM [Vimont et al., 2003; Chang et al., 2007]. During the 1997/1998 event (Figure 3c), negative values of the NPO index and positive values of the PMM SST and wind indices were observed before and during the onset of the event (November 1996 to May 1997). However, the NPO forcing and PMM coupling that favor the development of the CP El Niño were not sustained into the following boreal summer and autumn. In contrast, the favorable NPO and PMM conditions lasted much longer for the 2015/2016 event (Figure 3d), during which large negative values of the NPO index and positive values of PMM SST and wind indices persisted from the boreal winter preceding the onset of the event into the following autumn (January–October 2015). This long-lasting subtropical forcing and subtropical Pacific coupling enabled the strong CP El Niño dynamics to sustain large positive SST anomalies in the tropical central Pacific throughout the 2015/2016 event.

Our analysis indicates that the CP El Niño dynamics has a stronger influence on the 2015/2016 event than on the 1997/1998 event. This explains why the maximum SST anomalies in the former event were displaced westward compared to those in the latter event (see Figure 1c). Since the subtropical forcing lasted into boreal autumn 2015, the CP El Niño SST anomalies continued to persist around the International Date Line via local air-sea interactions during the following two seasons. No such forcing existed during the decaying phase of the 1997/1998 event. Therefore, these two events were very different in their SST evolution during their decaying phases.

3.3. Distinct North American Impacts of the 1997/1998 and 2015/2016 Events

During the decaying phase in boreal spring (March–May), positive precipitation anomalies were large and covered all of the tropical central-to-eastern Pacific in the 1997/1998 event (Figures S2a–S2c) but were

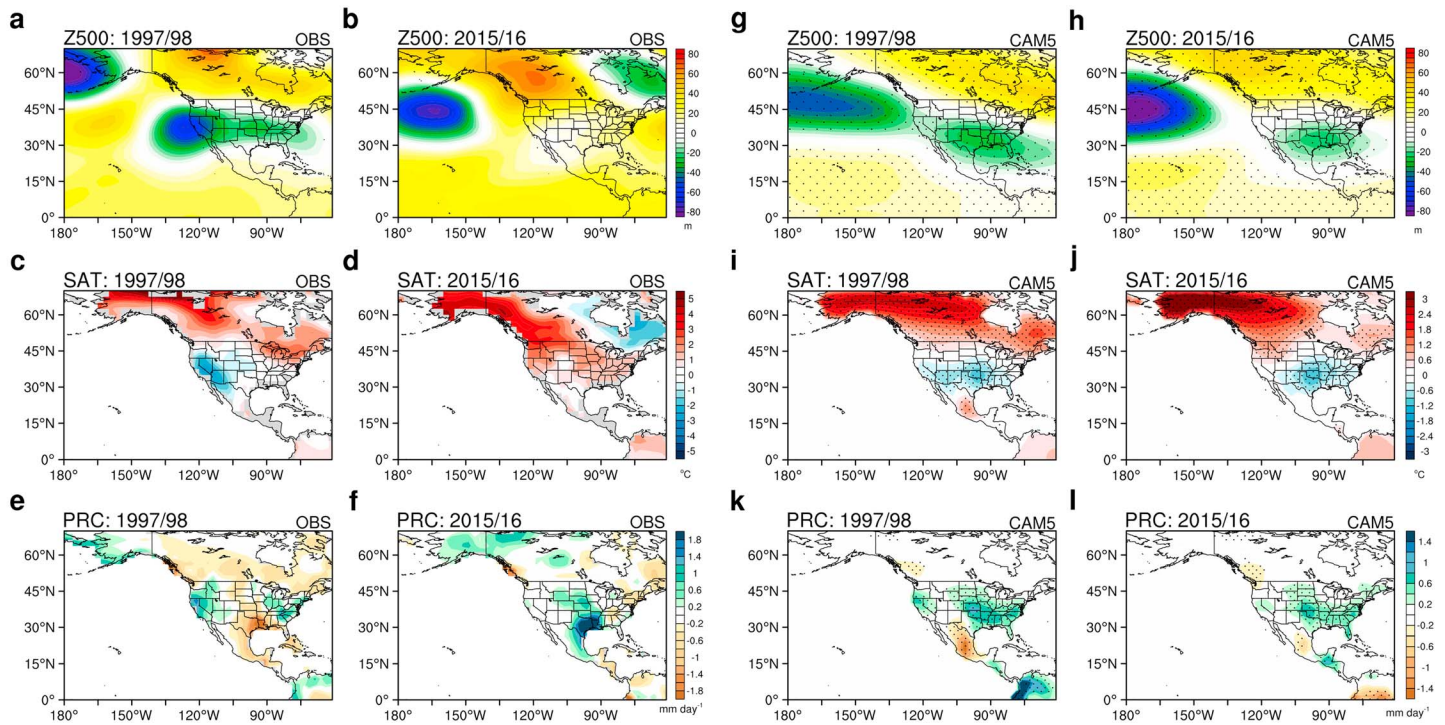


Figure 4. The observed 500 hPa geopotential height (Z500) anomalies during the decaying spring (March–May) for (a) the 1997/1998 event and (b) the 2015/2016 event. (c, d) As in Figures 4a and 4b but for the surface air temperature (SAT) anomalies. (e, f) As in Figures 4a and 4b but for the precipitation (PRC) anomalies. (g–l) As in Figures 4a–4f but for the CAM5 model simulations.

small and confined to the west of 150°W anomalies in the 2015/2016 event (Figures S2d–S2f). The precipitation pattern during the 1997/1998 event is similar to the typical pattern associated with the EP El Niño, whereas the pattern during the 2015/2016 event is similar to that associated with the CP El Niño [Kao and Yu, 2009]. The different heating patterns associated with these different precipitation anomalies can excite different wave train patterns propagating into midlatitudes resulting in different impacts on North American climate [e.g., Yu *et al.*, 2012b]. During the 1997/1998 event (Figure 4a), the 500 hPa geopotential height anomaly pattern is characterized by positive anomalies in the tropical central-to-eastern Pacific (180°–90°W, 0°–15°N), negative anomalies off the West Coast of North America extending toward the East Coast, and another positive anomalies over northern North America/Canada extending to Hudson Bay. This pattern is similar to that of the tropical Northern Hemisphere (TNH) [Mo and Livezey, 1986] pattern. During the 2015/2016 event (Figure 4b), the height anomaly pattern is characterized by positive anomalies over the tropical central Pacific (180°–150°W, 0°–15°N), negative anomalies near the Aleutian Islands, and another positive anomalies over northwestern North America. This wave train pattern is similar to that of the Pacific-North American (PNA) pattern. These results are consistent with the suggestion of Yu *et al.* [2012b] that the EP El Niño excites the TNH pattern, and the CP El Niño excites the PNA pattern. The different wave train patterns caused the surface temperatures to be colder than normal across the United States (U.S.) during the 1997/1998 event (Figure 4c) but warmer than normal during the 2015/2016 event (Figure 4d). The difference is quite dramatic in the western U.S., where the extremely cold spring during the 1997/1998 event contrasts with the warmer-than-normal spring during the 2015/2016 event (Figure S3b). The wave train patterns also enable El Niño events to affect the rainfall patterns over U.S. by displacing the locations of the tropospheric jet streams that steer the paths of winter storms. Due to the different wave trains, the excessive rainfall received by the western U.S. during the spring of the 1997/1998 event (Figure 4e) was not seen during the spring of the 2015/2016 event (Figure 4f). Instead, the wave train pattern during the 2015/2016 event created an anomalous ridge off the West Coast of North America (see Figures 4b and S3a), which prevented the southward displacement of the jet streams resulting in near-normal rainfall in much of the western U.S. [e.g., Seager *et al.*, 2015].

We performed numerical experiments using the NCAR Community Atmosphere Model version 5 (CAM5) to further confirm the above observation-based findings on the different impacts of the 1997/1998 and 2015/2016 El Niño events. We conducted 50 member ensemble experiments driven by climatological and annually cycled SSTs by adding SST anomalies of 1997/1998 and 2015/2016 El Niño events, respectively, over the tropical Pacific (20°S–20°N, 120°E to the American Coast; see Figures S2d and S2e). The simulation results during boreal spring (Figures 4g–4l and S3d–S3f) show some consistency with those from the observations (cf. Figures 4a–4f and S3a–S3c), although the simulated anomalies are weaker than observed. The SST forcing of the 1997/1998 event produces negative height anomalies off the West Coast of North America extending across the entire U.S. that brings statistically significant anomalously cold and wet conditions to the western U.S. (Figures 4g, 4i, and 4k). In contrast, the westward displaced SST forcing during the 2015/2016 event produces a negative height anomaly center around Aleutian Islands and near-normal height anomalies off West Coast of North America (compared to the 1997/1998 event), leading to the different (from the 1997/1998 event) temperature and precipitation anomalies in the western U.S. (Figures 4h, 4j, 4l, and S3d–S3f). Nonsignificant temperature anomalies simulated in the southern part of the western U.S. (Figures 4j) are the result of the simulated positive height anomalies over the northwestern North America (Figures 4h) that do not extend southward as much as the observed (cf. Figures 4d and 4b). Outside the western U.S., nontrivial differences between observations and model simulations for the 2015/2016 event exist. For example, the simulated height and temperature anomalies in the southeastern U.S. are more negative than the observed. The simulated precipitation anomalies are drier over Texas and wetter in the southeastern U.S. These model biases might be related to tropical Atlantic SST anomalies [Kushnir *et al.*, 2010] or subtropical western Pacific SST anomalies [Lau *et al.*, 2006] which are not included in our simulations.

Hoell *et al.* [2016] also examined November–April California precipitation during El Niño events using a large (130) ensemble of Atmospheric Model Intercomparison Project simulations. They concluded that the strong El Niño events increase greatly the probability of wet conditions in California, while near-to-below-average California precipitation during such events is also a possible outcome of low probability. Therefore, the different impacts of the 1997/1998 and 2015/2016 events on California precipitation can be a result of internal variability. It should be pointed out that our study used atmospheric model simulations forced by El Niño-associated SST anomalies only in the tropical Pacific to isolate possible influences from other regions and showed that two extreme El Niño events with different longitudinal locations of tropical Pacific SST anomalies can lead to some differences in midlatitude rainfall/teleconnection patterns during boreal spring. Our study adds another possible explanation, in addition to the internal variability that Hoell *et al.* [2016] suggested, for why these two extreme El Niño events produce different impacts on California climate.

4. Conclusion and Discussion

Within a framework that emphasizes the two types of El Niño, we are able to show in this study that the two strongest extreme El Niño events on record (i.e., the 1997/1998 and 2015/2016 events) are very different in terms of their underlying dynamics and climate impacts, contrary to the popular view that these two events were similar. We find that the 1997/1998 event evolved in a way that suggests that it was dominated by the EP El Niño dynamics, while the evolution of the 2015/2016 event suggests that a mixture of both the EP and CP El Niño dynamics was at work. The stronger influence of the CP El Niño dynamics caused the 2015/2016 event to deviate from the 1997/1998 event, particularly during their decaying phases. The difference also enables us to explain, at least partially, why the impacts of the 1997/1998 event on the U.S. climate (e.g., western U.S. rainfall and temperatures) were not repeated during the 2015/2016 event. These results indicate that the increasing importance of the CP El Niño dynamics during the past two decades [e.g., Yu *et al.*, 2012a, 2012b, 2015; Capotondi *et al.*, 2015] is still ongoing, and this trend has even influenced the properties and climate impacts of extreme El Niño events. Our results challenge the recent view that extreme El Niño events have a similar underlying dynamics of EP type [Takahashi *et al.*, 2011; Cai *et al.*, 2015]. The present study shows that extreme El Niño events can occur without being a pure EP type as usually thought, and that triggering mechanisms and evolution can differ from event to event. Moreover, separating El Niño events into the EP and CP types helps to better understand the differences among extreme El Niño events.

It should be noted that our study does not consider the possible impact of the weak 2014/2015 El Niño on the development of the 2015/2016 El Niño suggested by Levine and McPhaden [2016], which was not present

prior to the 1997/1998 El Niño and can be another reason for the differences between the two events. While this study mainly focuses on the connections among subtropical atmospheric forcing, the PMM and the CP type of El Niño, other studies have suggested that the PMM-associated surface wind anomalies can excite downwelling Kelvin waves along the equatorial thermocline that propagate eastward to trigger EP El Niño events [e.g., Alexander *et al.*, 2010; Anderson and Perez, 2015]. Capotondi and Sardeshmukh [2015] have also shown that initial thermocline conditions play a key role in the development of an incipient tropical warming into either a CP or an EP type of ENSO event.

Acknowledgments

The authors thank two anonymous reviewers and Editor Kim Cobb for their very constructive comments that have helped improve the paper. This work was supported by the National Science Foundation's Climate and Large Scale Dynamics Program under grants AGS-1233542 and AGS-1505145. We would like to acknowledge high-performance computing support from Yellowstone provided by NCAR's Computational and Information Systems Laboratory, sponsored by the National Science Foundation. The model simulation data used in this study are available from the authors upon request (paekh@uci.edu or jyyu@uci.edu)

References

- Alexander, M. A., D. J. Vimont, P. Chang, and J. D. Scott (2010), The impact of extratropical atmospheric variability on ENSO: Testing the seasonal footprinting mechanism using coupled model experiments, *J. Clim.*, *23*, 2885–2901.
- Anderson, B. T., and R. C. Perez (2015), ENSO and non-ENSO induced charging and discharging of the equatorial Pacific, *Clim. Dyn.*, *45*, 2309–2327.
- Ashok, K., S. K. Behera, S. A. Rao, H. Weng, and T. Yamagata (2007), El Niño Modoki and its possible teleconnection, *J. Geophys. Res.*, *112*, C11007, doi:10.1029/2006JC003798.
- Battisti, D. S., and A. C. Hirst (1989), Interannual variability in the tropical atmosphere-ocean model: Influence of the basic state, ocean geometry and nonlinearity, *J. Atmos. Sci.*, *45*, 1687–1712, doi:10.1175/1520-0469%281989%29046<1687%3AIVIATA>2.0.CO;3B2.
- Cai, W., *et al.* (2015), ENSO and greenhouse warming, *Nat. Clim. Change*, *5*, 849–859, doi:10.1038/nclimate2743.
- Capotondi, A. (2013), ENSO diversity in the NCAR CCSM4 climate model, *J. Geophys. Res. Oceans*, *118*, 4755–4770, doi:10.1002/jgrc.20335.
- Capotondi, A., and P. D. Sardeshmukh (2015), Optimal precursors of different types of ENSO events, *Geophys. Res. Lett.*, *42*, 9952–9960, doi:10.1002/2015GL066171.
- Capotondi, A., *et al.* (2015), Understanding ENSO diversity, *Bull. Am. Meteorol. Soc.*, *96*, 921–938, doi:10.1175/BAMS-D-13-00117.1.
- Chang, P., L. Zhang, R. Saravanan, D. J. Vimont, J. C. H. Chiang, L. Ji, H. Seidel, and M. K. Tippett (2007), Pacific meridional mode and El Niño–Southern Oscillation, *Geophys. Res. Lett.*, *34*, L16608, doi:10.1029/2007GL030302.
- Chen, M., P. Xie, J. E. Janowiak, and P. A. Arkin (2002), Global land precipitation: A 50-yr monthly analysis based on gauge observations, *J. Hydrometeorol.*, *3*, 249–266, doi:10.1175/1525-7541(2002)003<0249:GLPAYM>2.0.CO;2.
- Chiang, J. C. H., and D. J. Vimont (2004), Analogous Pacific and Atlantic meridional modes of tropical atmosphere-ocean variability, *J. Clim.*, *17*, 4143–4158, doi:10.1175/JCLI4953.1.
- Dee, D. P., *et al.* (2011), The ERA-Interim reanalysis: Configuration and performance of the data assimilation system, *Q. J. R. Meteorol. Soc.*, *137*, 553–597, doi:10.1002/qj.828.
- Hoell, A., M. Hoerling, J. Eischeid, K. Wolter, R. Dole, J. Perlwitz, T. Xu, and L. Cheng (2016), Does El Niño intensity matter for California precipitation?, *Geophys. Res. Lett.*, *43*, 819–825, doi:10.1002/2015GL067102.
- Jin, F.-F. (1997), An equatorial recharge paradigm for ENSO, I. Conceptual model, *J. Atmos. Sci.*, *54*, 811–829, doi:10.1175/1520-0469(1997)054<0811:AEORPF>2.0.CO;2.
- Kalnay, E., *et al.* (1996), The NCEP/NCAR 40-year reanalysis project, *Bull. Am. Meteorol. Soc.*, *77*, 437–471, doi:10.1175/1520-0477(1996)077<0437:TNYRP>2.0.CO;2.
- Kao, H. Y., and J.-Y. Yu (2009), Contrasting Eastern-Pacific and Central-Pacific types of ENSO, *J. Clim.*, *22*, 615–632, doi:10.1175/2008JCLI2309.1.
- Kim, S. T., J.-Y. Yu, A. Kumar, and H. Wang (2012), Examination of the two types of ENSO in the NCEP CFS model and its extratropical associations, *Mon. Weather Rev.*, *140*, 1908–1923, doi:10.1175/MWR-D-11-00300.1.
- Kug, J.-S., F.-F. Jin, and S.-I. An (2009), Two types of El Niño events: Cold tongue El Niño and warm pool El Niño, *J. Clim.*, *22*, 1499–1515, doi:10.1175/2008JCLI2624.1.
- Kushnir, Y., R. Seager, M. Ting, N. Naik, and J. Nakamura (2010), Mechanisms of tropical Atlantic SST influence on North American precipitation variability, *J. Clim.*, *23*, 5610–5628.
- Larkin, N. K., and D. E. Harrison (2005), On the definition of El Niño and associated seasonal average U.S. weather anomalies, *Geophys. Res. Lett.*, *32*, L13705, doi:10.1029/2005GL022738.
- Lau, N.-C., A. Leetmaa, and M. J. Nath (2006), Attribution of atmospheric variations in the 1997–2003 period to SST anomalies in the Pacific and Indian Ocean basins, *J. Clim.*, *19*, 3607–3628.
- Lee, T., and M. J. McPhaden (2010), Increasing intensity of El Niño in the central-equatorial Pacific, *Geophys. Res. Lett.*, *37*, L14603, doi:10.1029/2010GL044007.
- Levine, A. F. Z., and M. J. McPhaden (2016), How the July 2014 easterly wind burst gave the 2015–2016 El Niño a head start, *Geophys. Res. Lett.*, *43*, 6503–6510, doi:10.1002/2016GL069204.
- Lin, C.-Y., J.-Y. Yu, and H. H. Hsu (2015), CMIP5 model simulations of the Pacific meridional mode and its connection to the two types of ENSO, *Int. J. Climatol.*, *35*, 2352–2358, doi:10.1002/joc.4130.
- Mo, K. C., and R. E. Livezey (1986), Tropical-extratropical geopotential height teleconnections during the Northern Hemisphere winter, *Mon. Weather Rev.*, *114*, 2488–2515.
- Rayner, N. A., *et al.* (2003), Global analyses of sea surface temperature, sea ice, and night marine air temperature since the late nineteenth century, *J. Geophys. Res.*, *108*(D14), 4407, doi:10.1029/2002JD002670.
- Rogers, J. C. (1981), The North Pacific Oscillation, *Int. J. Climatol.*, *1*, 39–57, doi:10.1002/joc.3370010106.
- Saha, S., *et al.* (2006), The NCEP climate forecast system, *J. Clim.*, *19*, 3483–3517, doi:10.1175/JCLI3812.1.
- Seager, R., M. Hoerling, S. Schubert, H. Wang, B. Lyon, A. Kumar, J. Nakamura, and N. Henderson (2015), Causes of the 2011 to 2014 California drought, *J. Clim.*, *28*(18), 6997–7024, doi:10.1175/JCLI-D-14-00860.1.
- Smith, T. M., R. W. Reynolds, T. C. Peterson, and J. Lawrimore (2008), Improvements to NOAA's Historical Merged Land–Ocean Surface Temperature Analysis (1880–2006), *J. Clim.*, *21*, 2283–2296, doi:10.1175/2007JCLI2100.1.
- Suarez, M. J., and P. S. Schopf (1988), A delayed action oscillator for ENSO, *J. Atmos. Sci.*, *45*, 3283–3287, doi:10.1175/1520-0469%281988%29045<3283%3AADA0FE>2.0.CO;3B2.
- Takahashi, K., A. Montecinos, K. Goubanova, and B. Dewitte (2011), ENSO regimes: Reinterpreting the canonical and Modoki El Niño, *Geophys. Res. Lett.*, *38*, L10704, doi:10.1029/2011GL047364.

- Vimont, D. J., J. M. Wallace, and D. S. Battisti (2003), The seasonal footprinting mechanism in the Pacific: Implications for ENSO, *J. Clim.*, *16*, 2668–2675, doi:10.1175/1520-0442(2003)16<2668%3ATSFMIT>2.0.CO;3B2.
- Walker, G. T., and E. W. Bliss (1932), World weather V Mem, *R. Meteorol. Soc.*, *4*, 53–84.
- Wyrtki, K. (1975), El Niño—The dynamic response of the equatorial Pacific Ocean to atmospheric forcing, *J. Phys. Oceanogr.*, *5*, 572–584, doi:10.1175/1520-0485(1975)5<29005<0572%3AENTDRO>2.0.CO;3B2.
- Xie, P., and P. A. Arkin (1997), Global precipitation: A 17-year monthly analysis based on gauge observations, satellite estimates, and numerical model outputs, *Bull. Am. Meteorol. Soc.*, *78*, 2539–2558.
- Yu, J.-Y., and H.-Y. Kao (2007), Decadal changes of ENSO persistence barrier in SST and ocean heat content indices: 1958–2001, *J. Geophys. Res.*, *112*, D13106, doi:10.1029/2006JD007654.
- Yu, J.-Y., and S. T. Kim (2010), Identification of Central-Pacific and Eastern-Pacific types of ENSO in CMIP3 models, *Geophys. Res. Lett.*, *37*, L15705, doi:10.1029/2010GL044082.
- Yu, J.-Y., and S. T. Kim (2011), Relationships between extratropical sea level pressure variations and the Central-Pacific and Eastern-Pacific types of ENSO, *J. Clim.*, *24*, 708–720, doi:10.1175/2010JCLI3688.1.
- Yu, J.-Y., H.-Y. Kao, and T. Lee (2010), Subtropics-related interannual sea surface temperature variability in the equatorial central Pacific, *J. Clim.*, *23*, 2869–2884, doi:10.1175/2010JCLI3171.1.
- Yu, J.-Y., M.-M. Lu, and S. T. Kim (2012a), A change in the relationship between tropical central Pacific SST variability and the extratropical atmosphere around 1990, *Enviro. Res. Lett.*, *7*, 034025, doi:10.1088/1748-9326/7/3/034025.
- Yu, J.-Y., Y. Zou, S. T. Kim, and T. Lee (2012b), The changing impact of El Niño on US winter temperatures, *Geophys. Res. Lett.*, *39*, L15702, doi:10.1029/2012GL052483.
- Yu, J.-Y., P.-K. Kao, H. Paek, H.-H. Hsu, C.-W. Hung, M.-M. Lu, and S.-I. An (2015), Linking emergence of the Central-Pacific El Niño to the Atlantic Multi-decadal Oscillation, *J. Clim.*, *28*, 651–662, doi:10.1175/JCLI-D-14-00347.1.



Geophysical Research Letters

Supporting Information for

Why were the 2015/16 and 1997/98 Extreme El Niños different?

Houk Paek^{1*}, Jin-Yi Yu¹, and Chengcheng Qian²

¹Department of Earth System Science, University of California, Irvine, California, USA

²Department of Marine Technology, College of Information Science and Engineering, Ocean University of China, Qingdao, China

*Corresponding Author: Dr. Houk Paek (paekh@uci.edu)

Contents of this file

Figures S1 to S3

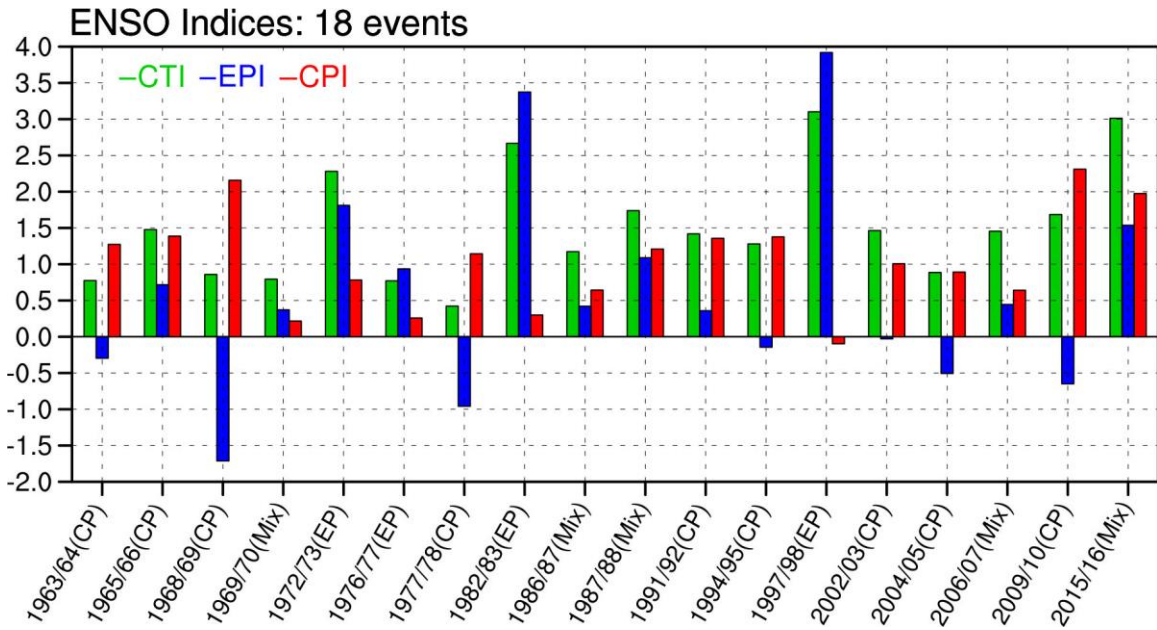


Figure S1. The CTI (standardized), EPI and CPI during the peak phases of the 18 El Niño events (that fulfill the NOAA’s criterion of the Ocean Niño Index being greater than or equal to 0.5 °C for a period of at least five consecutive and overlapping three-month seasons). The El Niño type of individual events is determined as a pure EP (CP) type when an EPI (CPI) is greater than the other index by 0.5, otherwise as a mixed type.

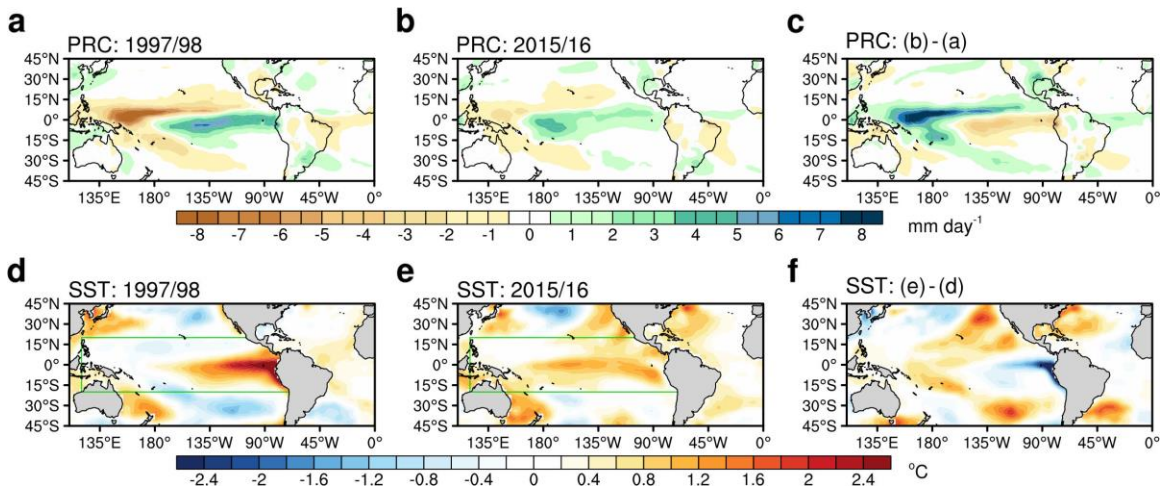


Figure S2. The precipitation (PRC) anomalies during the decaying spring (March-May) for (a) the 1997/98 event, (b) the 2015/16 event, and (c) their difference. (d)-(f) As in (a)-(c) but for the SST anomalies. The green boxes in (d) and (e) denote the domains in which SST anomalies have been prescribed in the model simulations.

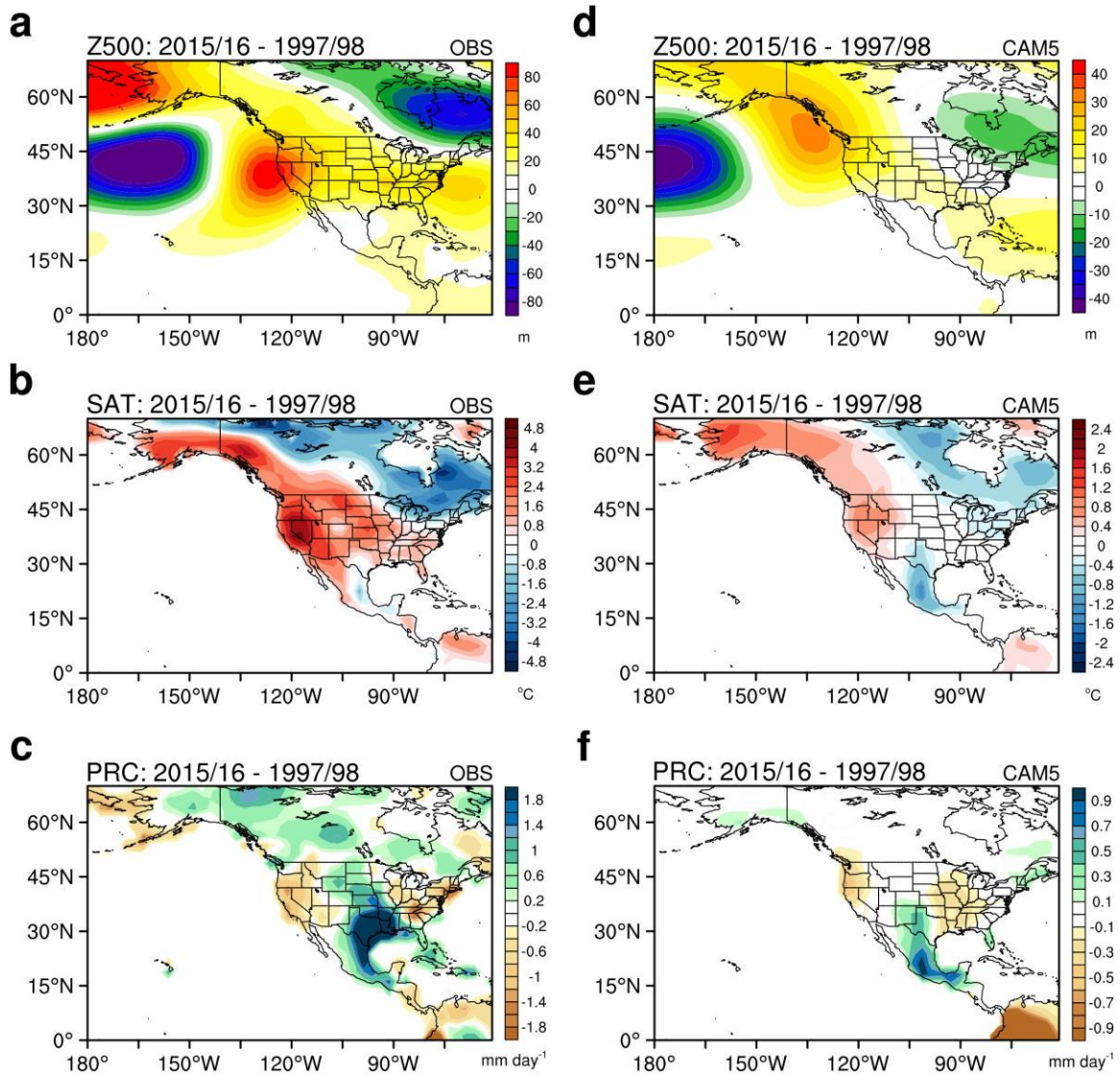


Figure S3. (a) The differences in the observed 500-hPa geopotential height (Z500) anomalies during the decaying spring (March-May) between the 2015/16 and 1997/98 events. (b), (c) As in (a) but for the surface air temperature (SAT) and precipitation (PRC) anomalies, respectively. (d)-(f) As in (a)-(c) but for the CAM5 model simulations.